Localization pitfalls of seismic events due to anisotropy – A KTB real data case study

K. Sommer, D. Gajewski, and R. Patzig

email: *sommer@dkrz.de, gajewski@dkrz.de*

keywords: *induced seismicity, localization, anisotropy*

ABSTRACT

The environment of the German Continental Deep drilling site (KTB) is known to be anisotropic. In this study we have analyzed the seismic events generated by the KTB long term injection experiment. More than 2500 seismic events were generated and about 260 events were recorded by the borehole geophone and by the 42 station surface array centered at the KTB. For this experiment we are in the favorable position to have a priori knowledge, where the acoustic emissions should originate, i.e., they should start at the injection point and slowly propagate away from it. Localizing the events using an isotropic model based on average velocities derived from check shots leads to a southward lateral shift of the center of the event cloud of about 500m away from the injection point. Since the total extension of the elongated event cluster is about 2 km in E-W direction and about 300-400 m in N-S direction this is a significant contribution. Using the 3-D isotropic velocity model obtained from the KTB reflection data, no significant change in the localization is observed and the lateral shift is reproduced. Localizing the same events using an anisotropic model based on published data centers the event cloud around the injection point. The anisotropic localization not only removes the lateral shift of the events but it also significantly alters the shape of the event cloud from an elongated cluster to an almost circular distribution. This is important if the spatio-temporal evolution is interpreted with respect to the hydraulic properties of the rocks. Also, interpretations with respect to event clustering due to tectonics or hydro-fracking may be severely affected if the localization is based on the wrong model assumptions. In seismology, most often there is no a priori information on the subsurface available and we are in a less favorable position than for the KTB injection experiment. A dislocation of the events due to anisotropy may be overlooked leading to the mis-interpretation of the distribution of the events and its spatio-temporal evolution.

INTRODUCTION

The problem of earthquake location is one of the most basic problems in seismology. Although numerous applications exist worldwide, the inherent non-linearity prevents earthquake location and tomography from being a standardized routine tool. The general strategy of most applications is the minimization of travel-time differences between observed and measured data. Currently they all have in common that an isotropic subsurface model is assumed. It is, however, known from seismological studies and reflection seismology that the earth is not isotropic. This anisotropy affects the localization of seismicity. In this study we quantify this effect for the hydraulically-induced seismic events of the KTB injection experiment. A fluid injection experiment provides perfect conditions for a real data case study since a priori knowledge on the event location is available. The events should start close to the injection point and propagate away from it with increasing injection time. The subsurface of the KTB is known to be anisotropic (Rabbel (1994) and Rabbel et al. (2004)) and provides therefore an ideal environment for this study.

We used a localization technique recently developed at the University of Hamburg. It allows to consider 3D-heterogeneous isotropic and anisotropic models. This technique is based on a grid search and was

verified using synthetic data before it was applied on the KTB data for this study. It shows that the neglect of anisotropy can lead to serious mis-localizations and thus to mis-interpretation of the located events. We will first describe the KTB injection experiment before we briefly explain the localization method used. After this we discuss the anisotropy of the KTB and present results of localizations of the induced seismicity using isotropic and anisotropic subsurface models. Discussions and conclusions finalize the paper.

EXPERIMENT

During the KTB injection experiment performed in the year 2000, a total of more than 4000 m^3 of water were injected into the KTB during a period of 60 days. The entire borehole was pressurized. The purpose was to generate micro-seismicity around the openhole section at a depth of about 9 km to investigate hydraulic properties of the KTB. More than 2500 seismic events were generated (Baisch et al., 2002). The events were observed by a surface network, which consisted of 42 stations, including a borehole geophone which was placed in the pilot hole located 200 m to the west of the KTB at a depth of about 4 km (Fig. 1). The borehole geophone was recording at 1000 Hz sampling frequency, while the surface network operated at 200 Hz. Due to a leakage of the casing near 5 km in depth about 75 % of the water escaped at this level.

Using the Geiger method (Geiger (1910)) 237 events were localized by Baisch et al. (2002) assuming a

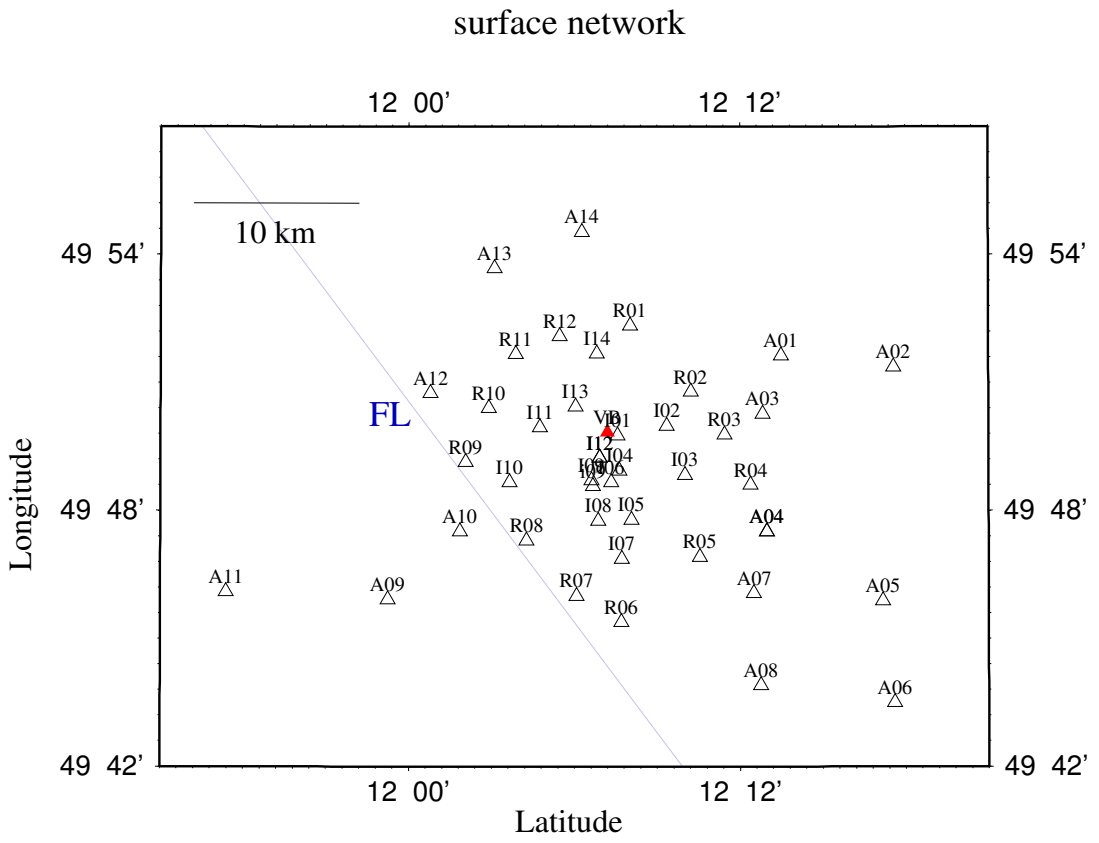

Figure 1: The arrangement of the surface network. The projection of the borehole geophone at the surface is marked by the red triangle. The blue line represents the Franconian Lineament as mapped at the surface.

homogeneous isotropic velocity model with mean velocities obtained from check shot data. Most of the events published in that work were located to the south of the injection (see Fig. 2). The events in 8 - 9 km depth are all east of the borehole. Station corrections were applied but are not quantified in the paper of Baisch et al. (2002). In the next section we will describe the localization technique used in this study.

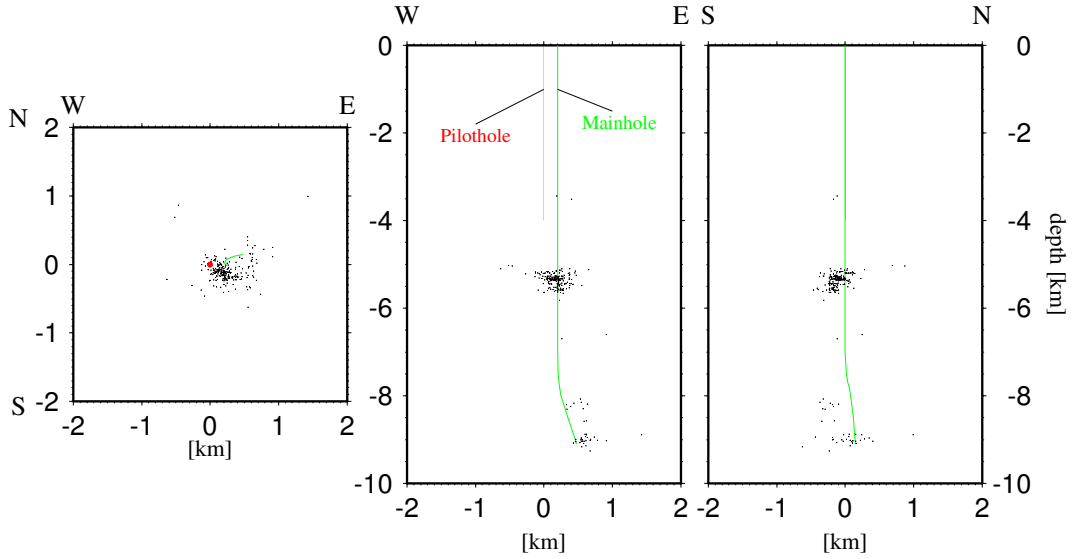

Figure 2: Localization of the events of the fluid injection experiment 2000 at the KTB as obtained by Baisch et al. (2002).

LOCALIZATION TECHNIQUE

Almost all technique currently used are minimizing an objective function based on the traveltime differences of observed and computed onset times of seismic events where an isotropic, and often homogeneous subsurface model is assumed. In the approach used here we minimize the residual square sum of the measured and the calculated traveltimes determined for different points within the discretized velocity model. The residual square sum provides a measure for the probability of the hypocenter to be located at the particular point in the model under consideration. The residual square sum R is defined as the square of the difference between measured and calculated P- and/or S-traveltimes at each station divided by the inaccuracy of the particular pick:

$$R = \sum_{m=1}^{M} \left(\frac{t^{(P)} - T^{(P)}}{\Delta t^{(P)}} \right)^2 + \left(\frac{t^{(S)} - T^{(S)}}{\Delta t^{(S)}} \right)^2 \quad , \tag{1}$$

where $T^{(P)}$ and $T^{(S)}$ are the computed P- and S onset times for the particular subsurface point. The traveltimes are computed using the velocity model under consideration which may be 3-D isotropic or anisotropic. The traveltimes $t^{(P)}$ and $t^{(S)}$ are the measured P- and S-onset times, m is the station number with $m = 1, 2, ..., M$, and M is the number of stations in the recording array which observed the event. The picking errors are specified by $\Delta t^{(P)}$ and $\Delta t^{(S)}$.

According to the equation above the hypocentral time, and thus the localization of the hypocenter, not only depend on the measured onset times, but also on the inaccuracies of the picks. Most localization methods apply some weights from 1 to 4 depending on the quality of the particular pick. We used the picks and weights as determined by Baisch et al. (2002). We converted their weights into picking errors according to Tab. 1.

Weight 1 corresponds to a picking error of one sample. This is 0.005 s for a station of the surface network and 0.001 s for the borehole geophone. Because of the higher signal to noise ratio of the borehole geophone the pick inaccuracy is always one sample. The theoretical traveltime is computed for every grid point of the discretized subsurface model. The maximum spacing of the subsurface grid should reflect the spatial bandwidth of the data. Model dimensions and computational limitations may require larger grid spacings. For model grids with spacings considerably larger than the average wavelength of the event under consideration locations between the grid nodes need to be considered. For these locations traveltime interpolation techniques are required that take the wavefront curvature into account to achieve higher accuracy, like the

weight	picking error [s]
1	0.005
2	0.010
3	0.025
4	0.050

Table 1: Conversion of weights into picking errors in ms.

hyperbolic interpolation technique of Vanelle and Gajewski (2002) . Because of the model dimensions of the KTB data the grid spacing of the subsurface model was up to 400 m.

For the computation of traveltimes on a 3-D grid various methods were established, like FD eikonal solvers (Vidale, 1988, 1990; Soukina et al., 2003), ray tracing methods (Vinje et al., 1996a,b; Coman and Gajewski, 2005; Kaschwich and Gajewski, 2003), shortest path (Moser, 1991), or bending techniques. See, e.g., Leidenfrost et al. (1999) for an overview of these techniques and their efficiencies. Quite often homogeneous models are still in use for event localization where analytical solutions can be applied.

After the traveltimes were generated, the node with the lowest residual square sum is considered as the hypocenter of the event under investigation. This minimum of the residual square sum is identified with a grid search algorithm. For this technique the values of the residual square sum at 27 points of a cube of the subsurface grid are evaluated during each step of the grid search procedure. If the central point shows the

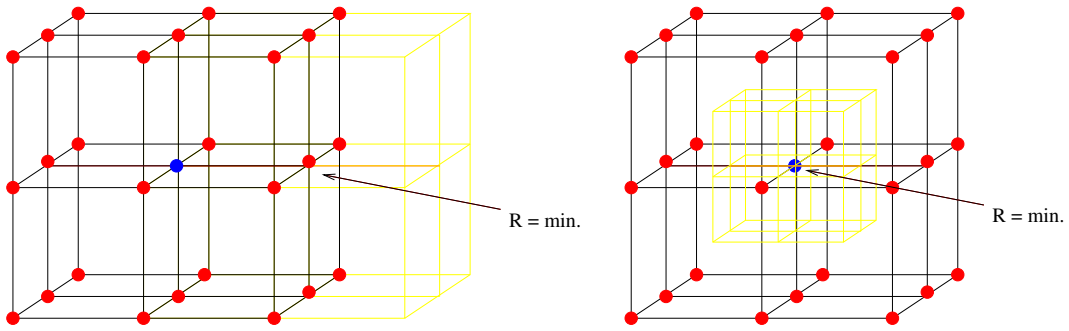

Figure 3: For the grid search procedure the residual square sums at 27 points of a cube of the subsurface grid are evaluated. If the central point of the cube shows the lowest value the cube is reduced to half its size. If one of the other points has the lowest value the cube is shifted so that this point now becomes the center of a new cube.

lowest value the cube shrinks to half of its size. If one of the other points displays the lowest value the cube moves such that this point becomes the center of the next cube to be investigated (Fig. 3). This procedure is continued until the size of the cube is below one characteristic wavelength, which corresponds to the maximum spatial resolution that can be achieved for event localization. The residuum at the minimum found in the way described above is a measure for the quality of the used model. The lower the residuum the better is the fit of the model to the data.

The technique described above can be used for homogeneous and heterogeneous, isotropic or anisotropic media. The grid search and traveltime interpolation are independent of the type of the model (i.e., 1-D, 2-D, 3-D isotropic or anisotropic), only the technique to compute traveltimes on the discretized subsurface grid needs to be adapted to the model under consideration. Therefore, the grid search approach provides a versatile procedure for event localization as it may be applied to different kinds of subsurface models without modification of the search itself. Since anisotropic models are the key issue of this paper we will review the anisotropy of the KTB environment in the following section.

SEISMIC ANISOTROPY AT THE KTB

After the pilothole was completed at the KTB site, a number of experiments were performed to determine the seismic anisotropy. The main results of these experiments were (Rabbel (1994); Rabbel et al. (2004)):

- The gneiss in the upper 3.5 km is anisotropic. The polarization direction of the faster shear wave coincides with the NW-SE-strike of the steeply-dipping rock foliation.
- In the depth interval from 2.2 - 3 km the anisotropy can be approximated by a hexagonal symmetry with a non vertical symmetry axis. It is mainly caused by the foliation of the gneiss, leading to an average anisotropy of 2.5 %, 14 % and 5 % for the P-, S1- and S2-wave, respectively.
- Zones of increased anisotropy correlate with zones of increased fracture density.
- The total anisotropy can be divided into two major components:
  - the intrinsic background anisotropy, related to mineral composition and foliation of gneiss,
  - the anisotropy caused by oriented fractures.
- Generally the KTB rocks displays azimuthal anisotropy, that is most often approximated by hexagonal symmetry with a non vertical symmetry axes.

Further information was obtained from the interpretation of VSP data collected during the years 1999 and 2000. These experiments focused on the lower part of the KTB (Rabbel et al. (2004)).
The upper and lower parts consist mainly of gneiss and show lower P-wave velocities (5.4 - 6.3 km/s) compared to the middle part that is dominated by amphibolite (6.3 - 6.8 km/s). Average S-wave velocities are 3.5 - 4.0 km/s and 3.3 - 3.6 km/s, respectively, for the gneiss and 3.6 - 4.0 km/s and 3.5 - 3.9 km/s, respectively, for the amphibolite. The main properties of the three observed depth levels are summarized as follows (Rabbel et al. (2004)):

- 2.2 - 3 km: the anisotropy of P-, S1- and S2-waves is 4.4 %, 9.0 % and 3.5 %, respectively. The average isotropic P- and S- wave velocities are 6.12 km/s and 3.15 km/s, respectively.
- middle section: the material is the same as in the shallower level. It shows 3.9 % lower average P-wave velocity (5.88 km/s) and 0.8 % lower average S-wave velocity (3.48 km/s), whereas the anisotropy increases (6.1 %, 11.7 % and 6.2 %, respectively).
- 7.9 - 8.2 km: we find a further decrease of the velocities and increase of anisotropy, namely 13.2 %, 18.3 % and 3.8 % for maximum estimates of the anisotropy of the P-, S1-, and S2-waves, respectively. The average isotropic velocities are 5.67 km/s and 3.37 km/s, respectively, for P- and S-waves.

While the velocity decreases in the lower part of the KTB the anisotropy increases at that depth. The anisotropy of the KTB environment is of orthorhombic or lower symmetry, but is usually approximated by a medium of hexagonal symmetry. The symmetry axis varies with depth where its orientation is tied to the geological structure, i.e. the symmetry axis is perpendicular to the foliation of the gneiss. The orientation of this foliation changes considerably with depth. Obviously, the anisotropy at the KTB is rather complicated and of remarkable magnitude. It affects the localization of seismic events which is considered in the next section.

RESULTS

Using a homogeneous isotropic model with average velocities determined from check shot data as published in Baisch et al. (2002) we obtained the localizations shown in Fig. 4. The center of the event cloud is shifted to the south by about 500 m. This corresponds to 25 % of the total extent of the event cloud. This is a physically unreasonable distribution of events since the center of the event cloud is not centered at the injection point but set off to the south. The localization of Baisch et al. (Fig. 2) could not be reproduced, since they used stations corrections that are not quantified in their paper. Station corrections are

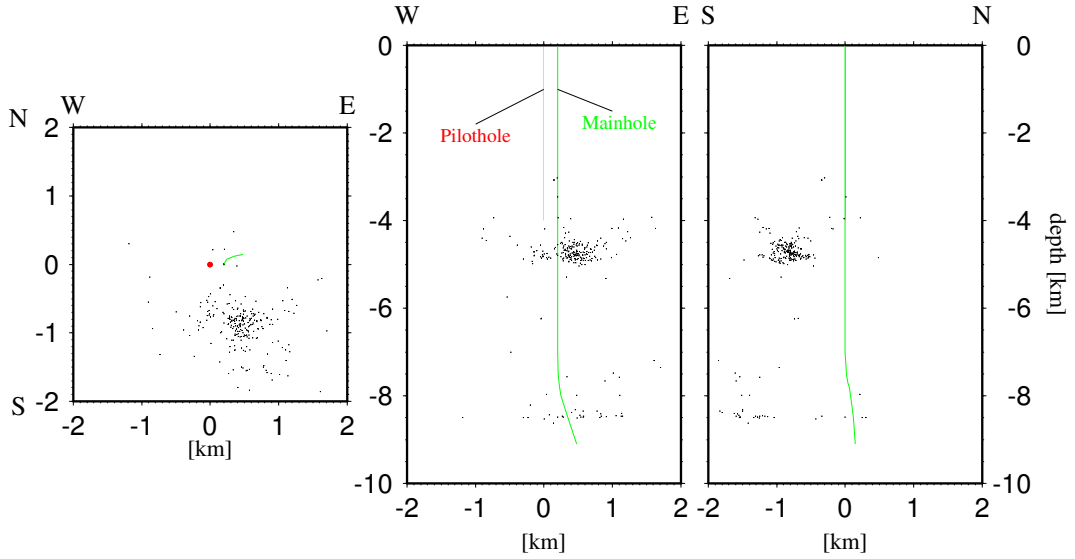

Figure 4: Localization with a homogeneous model (v_P=6080 m/s and v_S=3510 m/s). The center of the event cloud is shifted to the south of the injection point by about 500 m.

applied in seismology if local site effects are present below certain stations of the network (thus changing the geology below the array), similar to static corrections in the presence of topography. We think that station corrections are inappropriate for the KTB data, since almost all stations are on the same geological unit. Only for the three stations to the west of he Franconian Lineament station corrections may be considered. The effect, however, should be rather small, since only a very short segment of the total ray path is affected due to the small thickness of the sediments below these stations. Moreover, Baisch et al. (2002) also applied station weights, emphasizing the borehole geophone 10 times stronger for P-wave events and 7 times stronger for S-wave events compared to the surface stations. Overweighting the shorter raypaths of the borehole receiver reduces the dependence of the localizations on anisotropy since these effects are more pronounced for longer ray paths.

Using a 3D heterogeneous isotropic velocity model derived from the 3-D KTB reflection data (Buske (1999)), no significant change in the localization was observed. The lateral shift of the event cloud was still present also for this model. Other available localization tools were also applied to the data like SimulPS (Evans et al. (1994)) which is based on the well known Geiger method. This localization applied to the KTB data and the isotropic homogeneous model displays an even stronger lateral shift to the south of the center of the event cloud. To estimate the deviations between our isotropic homogeneous localization and the isotropic localizations of Baisch et al. (2002) with weights and station correctons we computed theoretical onset times for every station assuming the event originated at the borehole at 5 km depth. The isotropic homogeneous velocity model was used and the traveltimes were compared with the measured onset times. We found a systematical distribution of these differences (Fig. 5) which indicates a directional dependence, i.e., anisotropy.

Despite the 3-D complexity of the anisotropy at the KTB we consider here a homogeneous anisotropic model which is derived from laboratory data. We used the elastic parameters determined from experiments on KTB rock samples by Jahns et al. (1994).:

$$\underline{A} = \begin{pmatrix} 43.48 & 11.09 & 13.20 & 0.00 & -0.10 & 0.52 \\ & 41.27 & 14.93 & 0.11 & -0.00 & 0.33 \\ & & 33.28 & 0.39 & -0.96 & 0.00 \\ & & & 10.70 & 0.44 & -0.13 \\ & & & & 10.42 & 0.07 \\ & & & & & 15.65 \end{pmatrix} \quad (2)$$

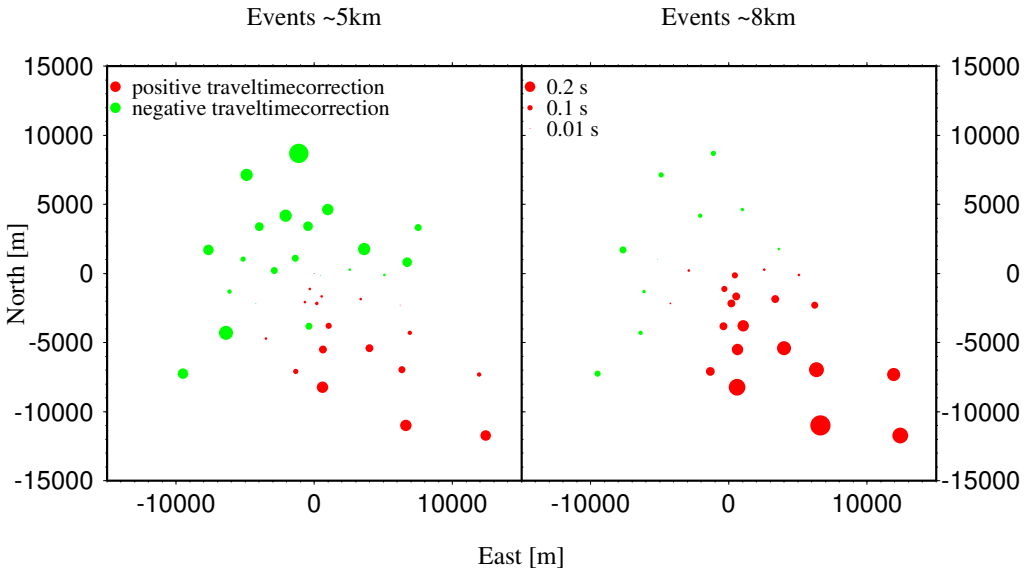

Figure 5: Differences of the onset times from the borehole to every station assuming the isotropic homogeneous velocity model and measured onset times. A systematic distribution of differences is obtained.

The elastic parameters of the investigated KTB rock sample correspond to a complex anisotropy with a symmetry lower than orthorhombic. The magnitude of the P-wave anisotropy is more than 10%. For the S-waves it is even stronger. The elastic tensor is given in its intrinsic coordinate system and had therefore to be rotated with respect to the geological situation and acquisition at the KTB (Fig. 6). The rotation was performed in a way that the fastest P-wave velocity of the anisotropic model is along the foliation of the gneiss and the slowest one perpendicular to it.

The localization of the data with this homogeneous anisotropic model leads to a physically reasonable distribution of events (Fig. 7), i.e., the event cloud is centered at the injection well. No station corrections or weights were applied. We observe from the isotropic and anisotropic localization, that not only the location of the events, but also the shape of the event cloud has changed considerably.

DISCUSSION AND CONCLUSIONS

The localization of the hydraulically induced seismicity of the KTB injection experiment using an isotropic homogeneous or a 3-D heterogeneous isotropic model show a strong lateral offset of the center of the event cloud to the south of the injection point. This is a physically unreasonable result. To locate the center of the event cloud at the injection point, the localization with isotropic models requires overweighting of the borehole geophone and station corrections . From several studies of the KTB subsurface it is known to be anisotropic. Magnitudes of more than 10% velocity anisotropy were reported. Our attempt to use an anisotropic model lead to a physically reasonable distribution of events, i.e., the center of the event cloud was located at the injection point. The anisotropic model used was determined from laboratory data and adjusted to the geological situation. For this localization neither station corrections nor station weights needed to be applied.

Although the anisotropic localization provides a physically reasonable result and is therefore the model of our preference, more work needs to be done. Residuals for both models, isotropic and anisotropic are still quite high. Statistically we can not even decide, which model is actually the better one since both lead to a similar quality of the fit. This disappointing conclusion is, however, not at all surprising since the geological situation and the anisotropy at the KTB is rather complex. This complexity is not appropriately reflected in the homogeneous anisotropic model. We would like to emphasize that careful velocity model building is essential for any localization, particularly if anisotropy is present: the quality obtained for a localization can never be better than the match of the used model to the real subsurface.

This data case study has demonstrated that the localization of events and the shape of the event cloud

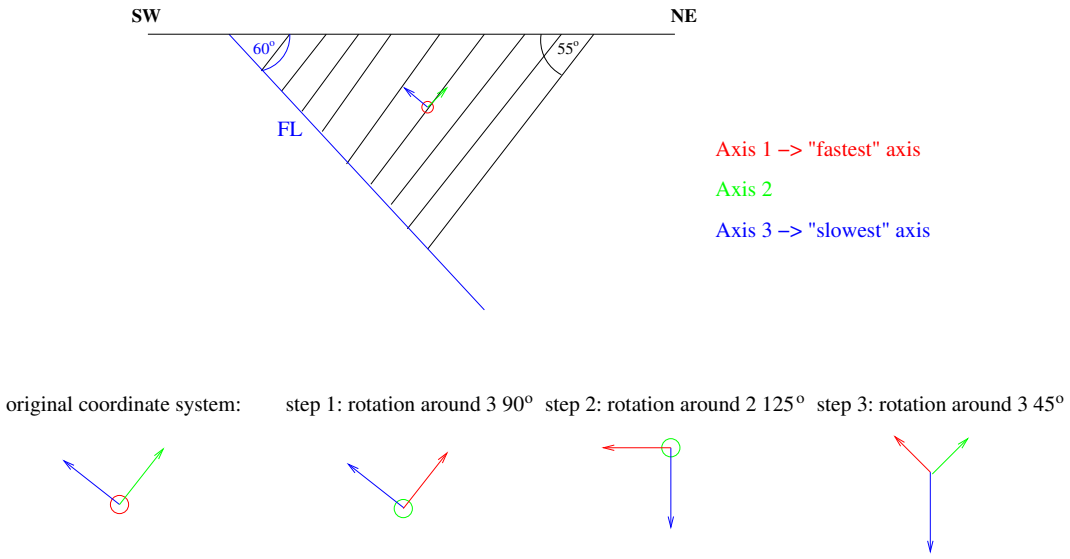

Figure 6: Rotation of the elastic tensor to fit the geologic situation. The KTB environment is characterized by steeply-dipping layers of gneiss with a pronounced foliation in the direction of the layering.

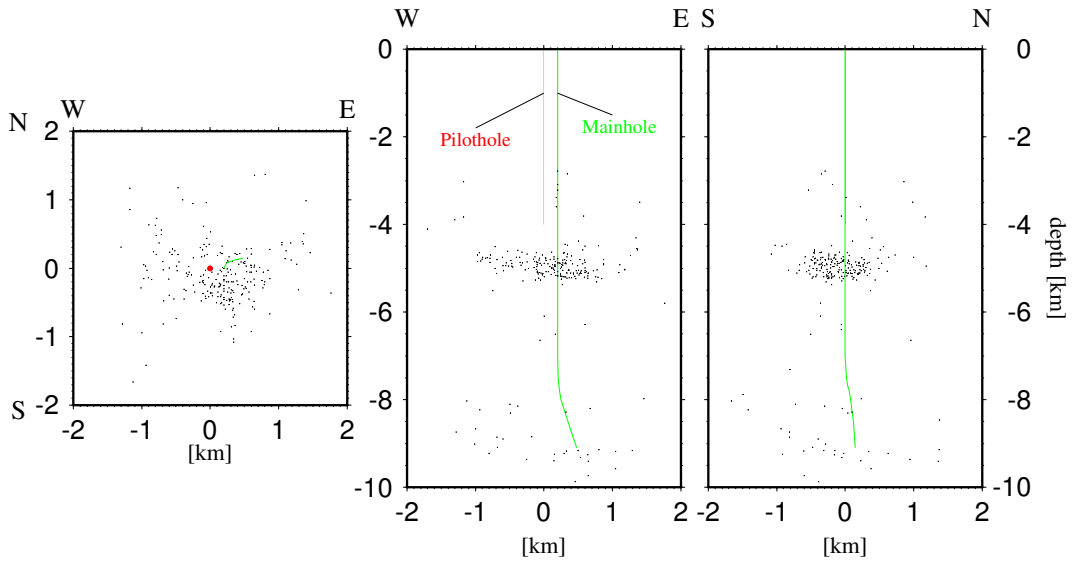

Figure 7: Localization with the homogeneous anisotropic velocity model. The cloud of events is centered around the borehole. The lateral shift of events observed for the isotropic model (Fig. 4) is not present. The shape of the cloud is now almost circular compared to the elongated shape obtained for the isotropic case (Fig. 4).

are strongly affected if a present anisotropy of the subsurface is neglected. In contrast to the injection experiment at the KTB in seismology we usually have no a priori information on the occurrence of events. We are therefore in a much less favorable position than in this study. A systematic displacement of the events due to an unidentified anisotropy may severely mislead the interpretation of the distribution of the events. Careful velocity model building including anisotropy prior to the localization is therefore mandatory.

ACKNOWLEDGMENTS

We are grateful to Svetlana Golovnina, Tina Kaschwich and Claudia Vanelle for discussions on the subject and for providing software to set up the anisotropic part of the localization. Claudia Vanelle also clarified several issues related to the statistics of residuals. We thank M. Bonhoff for providing the data including picks and localizations. This work was partially supported by the sponsors of the Wave Inversion Technology consortium and the DGMK (Deutsche Gesellschaft für Erdöl, Erdgs und Kohle) project 593-3.

REFERENCES

Baisch, S., Bohnhoff, M., Ceranna, L., Tu, Y., and Harjes, H.-P. (2002). Probing the Crust to 9 km depth: Fluid injections experiments and induced seismicity at the KTB superdeep drilling hole, Germany. *BSA*, 92:2369–2380.

Buske, S. (1999). Three-dimensional pre-stack Kirchhoff migration of deep seismic reflection data. *GJI*, 137:234–260.

Coman, R. and Gajewski, D. (2005). Traveltime computation by wavefront-oriented ray tracing. *Geophysical Prospecting, in press*.

Evans, J., Eberhart-Phillips, D., and Thurber, C. H. (1994). User's manual for simulps12 for imaging vp and vp/vs: A derivative of the "thurber" tomographic inversion simul3 for local earthquakes. *USGS Open-File Report 94-431*.

Geiger, L. (1910). Herdbestimmung bei Erdbeben aus den Ankunftszeiten. *K. Ges. Wiss. Gött.*, 4:331–349.

Jahns, E., Siegesmund, S., Rabbel, W., and Chlupac, T. (1994). Seismic Anisotropy: Comparison of Lab-, Logging, and VSP-Data. *KTB-Report 94-2*, pages A163–A167.

Kaschwich, T. and Gajewski, D. (2003). Wavefront-oriented ray tracing in 3D anisotropic media. In *Expanded Abstracts*, pages P–041. 65th EAGE Meeting and Technical Exhibition.

Leidenfrost, A., Ettrich, N., Gajewski, D., and Kosloff, D. (1999). Comparison of six different methods for calculating traveltimes. *Geophysical Prospecting*, 47:269–297.

Moser, T. J. (1991). Shortest path calculation of seismic rays. *GEO*, 56:59–67.

Rabbel, W. (1994). Seismic anisotropy at the Continental Deep Drilling Site (Germany). *Tectonophysics*, 232:329–341.

Rabbel, W., Beilecke, T., Bohlen, T., Fischer, D., Frank, A., Hasenclever, J., Borm, G., Kück, J., Bram, K., Druivenga, G., Lüschen, E., Gebrande, H., Pujol, J., and Smithson, S. (2004). Super-deep vertical seismic profiling at the KTB deep drill hole (Germany): Seismic close-up view of a major thrust zone down to 8.5 km depth. *GJR*, 109 (B9)(B09309).

Soukina, S., Gajewski, D., and Kashtan, B. (2003). Traveltime computation for 3-D anisotropic media by a finite-difference perturbation method. *Geophysical Prospecting*, 51:431–441.

Vanelle, C. and Gajewski, D. (2002). Second-order interpolation of traveltimes. *GP*, 50:73–83.

Vidale, J. (1988). Finite-difference calculation of traveltimes. *Bull. Seis. Soc. Am.*, 78:2062–2076.

Vidale, J. (1990). Finite-difference calculation of traveltimes in three dimensions. *Geophysics*, 55:521–526.

Vinje, V., Iversen, E., Åstebøl, K., and Gjøystdal, H. (1996a). Estimation of multivalued arrivals in 3D models using wavefront construction–Part I. *Geophys. Prosp.*, 44:819–842.

Vinje, V., Iversen, E., Åstebøl, K., and Gjøystdal, H. (1996b). Part II: Tracing and interpolation. *Geophys. Prosp.*, 44:843–858.